ARNOL'D TONGUES, THE DEVIL'S STAIRCASE, AND SELF-SIMILARITY IN THE DRIVEN CHUA'S CIRCUIT

by

Ladislav Pivka, Alexander L. Zheleznyak, and Leon O. Chua

Memorandum No. UCB/ERL M94/86

1 August 1994

ARNOL'D TONGUES, THE DEVIL'S STAIRCASE, AND SELF-SIMILARITY IN THE DRIVEN CHUA'S CIRCUIT

by

Ladislav Pivka, Alexander L. Zheleznyak, and Leon O. Chua

Memorandum No. UCB/ERL M94/86

1 August 1994

ELECTRONICS RESEARCH LABORATORY

College of Engineering
University of California, Berkeley
94720

ARNOL'D TONGUES, THE DEVIL'S STAIRCASE, AND SELF-SIMILARITY IN THE DRIVEN CHUA'S CIRCUIT

by

Ladislav Pivka, Alexander L. Zheleznyak, and Leon O. Chua

Memorandum No. UCB/ERL M94/86

1 August 1994

ELECTRONICS RESEARCH LABORATORY

College of Engineering
University of California, Berkeley
94720

ARNOL'D TONGUES, THE DEVIL'S STAIRCASE, AND SELF-SIMILARITY IN THE DRIVEN CHUA'S CIRCUIT

LADISLAV PIVKA, ALEXANDER L. ZHELEZNYAK, and LEON O. CHUA

Electronics Research Laboratory and
Department of Electrical Engineering and Computer Sciences
University of California, Berkeley
CA 94720, U. S. A.

Abstract

Empirical recurrent relations, governing the structure of the devil's staircase in the driven Chua's circuit are given, which reflect the self-similar structure in an algebraic form. In particular, it turns out that the same formulas hold for both winding and period numbers, but with different 'initial conditions'.

Some of the finer details such as period-doubling along with numerous coexistence phenomena within staircases of mode-locked states have been revealed by computing high-resolution bifurcation diagrams.

1. Introduction

One of the remarkable properties of nonlinear oscillators is their ability to lock onto certain subharmonic frequency when driven by an external source of energy. Associated with the phase-locking property is usually the appearance of staircases of phase-locked states when the parameters are varied over certain range. The picturesque name *devil's staircase* was coined by Mandelbrot [1977] to capture the intricate, often fractal, structure of such staircases. The devil's staircase was observed earlier [Harmon, 1961] in models of artificial neurons, although no laws describing its structure were formulated at that time. Since then the phenomenon has been reported from a large number of discrete or time-continuous, mostly one- or two-dimensional, forced dynamical systems. Attempts to describe the staircase structure of phase-locked states in an algebraic form led to the formulation of the period-adding law [Kaneko, 1983], and applications of Farey trees [Cvitanović, 1985].

The theory of mode-locked behavior is most developed for discrete 1-D maps since they are easier to investigate. Perhaps the most well-known example is the circle map [Jensen *et al.*, 1983, 1984; Ding & Hemmer, 1988]. Van der Pol's and the Duffing oscillators are classic examples of two-dimensional, continuous-time dynamical systems exhibiting a rich variety of dynamical behavior. The structure of bifurcations, frequency-lockings, and devil's staircases in these systems is still an active research area [Parlitz & Lauterborn, 1987; Rajasekar & Lakshmanan, 1988, 1992; Kaiser & Eichwald, 1991; Englisch & Lauterborn, 1991; Mettin *et al.*, 1993].

In circuit theory, the period-adding law and the devil's staircase have been observed in several second-order driven circuits [Chua *et al.*, 1986; Kennedy & Chua, 1986; Pei *et al.*, 1986; Luprano & Hasler, 1989; Kennedy *et al.*, 1989]. Among higher-dimensional systems, Chua's circuit has emerged as a paradigm for the generation of a multitude of dynamical behaviors [Chua *et al.*, 1993, Madan, 1993]. Its nonautonomous four-dimensional version has also been investigated [Murali & Lakshmanan, 1991, 1992, 1993a, 1993b]. The appearance of the devil's staircase is reported in Murali & Lakshmanan [1992] but its structure is not described in detail. Different mechanisms of transition to chaos, intermittency, forced synchronization, and other phenomena in the nonautonomous Chua's circuit are studied via two-parameter bifurcation diagrams in [Anishchenko *et al.*,1995].

Since Chua's circuit can be used to model the behavior of many other dynamical systems, the phenomena occuring in the nonautonomous circuit can be expected to be universal for a large class of dynamical systems. Therefore this contribution is devoted to the investigation of the driven Chua's circuit with a three-dimensional state space of variables.

2. Chua's Circuit as Excitable Dynamical System

Consider the circuit shown in Fig.1a, driven by an external current source $\bar{I}(t)$. We will use a sinusoidal input of the form $\bar{I}(t) = \bar{A}\ cos(\bar{w}t)$ with amplitude $\bar{A}$ and angular frequency $\bar{w}$.

The state equations for Chua's circuit can be written in the dimensionless form as follows [Madan, 1993]:

$$\left.\begin{aligned}\dot{x} &= \alpha(y - x - f(x)) + I(\tau)\\ \dot{y} &= x - y + z\\ \dot{z} &= -\beta y\end{aligned}\right\} \qquad (1)$$

where

$$f(x) = (1/2)\left[(s_2 + s_1)x + (s_0 - s_1)(|x - B_1| - |B_1|) + (s_2 - s_0)(|x - B_2| - |B_2|)\right]$$

is a three-segment piecewise-linear function obtained from that of Fig.1b through scaling, where the slopes m_0, m_1, m_2 are transformed into s_0, s_1, s_2, and $I(\tau) = A\ cos(w\tau)$. The breakpoints $B_1 = -1$ and $B_2 = 0.0234168$ as well as the paramater values $\alpha = 10$, $\beta = 0.3014987$, $s_1 = 0.078573$, $s_0 = -1.25719$, $s_2 = 55.78573$ will be fixed throughout the paper.

With zero excitation force $I \equiv 0$, the system is bistable with two stable equilibria P^+, P^-, while the origin is a saddle equilibrium point. The above parameter values are chosen so that a small external force I (e.g., for $A = -0.06$ and $w = 0$) can trigger the circuit into a stable oscillatory regime. It is apparent from Fig.2 that the cyclical regime is a highly relaxational one.[1] Also due to such character of oscillations, it was possible to write a simple computer routine to count and evaluate patterns in the local minima of the waveforms.

The relaxational property is a consequence of the strong asymmetry of the piecewise-linear function f, and has been successfully employed for the generation of triggered waves and spiral waves [Pérez-Muñuzuri *et al.*, 1993] in arrays of Chua's circuits. Many other interesting dynamical behaviors can be expected to occur in such arrays . However, as mentioned elsewhere [Anishchenko *et al.*], before embarking on a detailed study of arrays, it is highly desirable to perform a thorough analysis of the single component cell under the influence of an external excitation.

3. Description of the Staircase Tree

As early as in 1927, the phenomenon of frequency entrainment was observed by van der Pol and van der Mark [1927] in experiments with a neon bulb RC relaxation oscillator. When such a phenomenon occurs, steps of mode-locked states appear, which often form

[1] There is also a small stable limit cycle encircling the point $P^- = (-1.238\ ,0\ ,1.238)$. However, we will be concerned with the large stable limit cycle only.

sequences, or staircases, over certain parameter ranges. Let us recall some of the relevant definitions before describing such structures.

Given a frequency f_s of forcing, and the system's response frequency f_d, the corresponding *winding number* will be $W = f_s/f_d$. Restated in terms of periods, $W = T_d/T_s$ where T_s, T_d are the periods associated with f_s, f_d respectively.[2] Note that W is in general a fraction. However, for subharmonic responses whose period T_d is an integer multiple of the input signal period T_s, the winding number will be an integer. For the *period number* we will take the number of local minima, per least period, in the waveform of one of the state variables (x or y) chosen for this study. In general, another state variable may give a different period number. Note that the period number is always an integer. For the parameter values from Section 2, the system (1) can exhibit a variety of subharmonics as the amplitude and frequency are varied. The winding and period numbers corresponding to the chosen parameter values are therefore integers, and points in the $A - w$ parameter plane having the same winding and period numbers form connected regions, called *Arnol'd tongues*, which in turn group together to form a hierarchy of staircase levels, or staircase tree, which we describe as follows (Fig.3). Let the amplitude $A > 0.07$ be constant. Then there is a sequence of intervals (or steps) of frequencies w in which the winding and period numbers take on constant values. We first consider only winding numbers for simplicity, the description for period numbers being similar. The sequence of steps with winding numbers $(T_0, T_1, T_2, \ldots) = (1, 2, 3, \ldots)$ will be called a level-I staircase. Shown in Fig.3 are two steps from level-I staircase, namely those labeled $\frac{I}{1/1}$ and $\frac{I}{2/1}$. Between any two successive level-I steps $p < q$ there are two staircases of steps whose winding numbers are governed by the laws

$$q \rightarrow q + p \rightarrow q + 2p \rightarrow \ldots q + np \rightarrow \ldots \infty \ldots \rightarrow p \tag{2}$$

and

$$p \rightarrow p + q \rightarrow p + 2q \rightarrow \ldots p + nq \rightarrow \ldots \infty \ldots \rightarrow q \tag{3}$$

[2]This is how winding numbers are defined, e.g., in Rajasekar & Lakshmanan [1988]. Different authors use different names for this quantity. The above frequency ratio is sometimes called *normalized period* [Chua *et al.*, 1986; Luprano & Hasler, 1989]. At other times, *rotation number* is taken to be the ratio of the number of periods of the driving signal and the number of output signal pulses, per system cycle [Kennedy *et al.*, 1989], while the winding number in Murali & Lakshmanan [1992] is the inverse of the rotation number. The *torsion number* [Uezu & Aizawa, 1982; Parlitz & Lauterborn, 1985] is another quantity, sometimes also called (generalized) winding number.

It is a matter of convention which of the two staircases will be called a next-level staircase between p and q. For a level-II staircase we will choose the one described by (2), whereas (3) will be chosen for level-III stairs. In our particular situation (Fig.3) $p = 1$, $q = 2$, and $\frac{I}{2/1}, \frac{II}{3/2}, \frac{II}{4/3}, \ldots$ is the level-II staircase, whereas $\frac{II}{3/2}, \frac{III}{5/3}, \frac{III}{7/4}, \ldots$ is the level-III staircase between p and q.

Higher levels are defined similarly, with p, q being the successive steps from the preceding level. With these conventions, every level-l step ($l = 1, 2, \ldots$) is the first step for a level-$(l+1)$ staircase, and each staircase of level $l+1$ ascends from a higher step of level l toward a lower step of level l. A similar tree structure can be defined for staircases of period numbers, starting with sequence $(T_0, T_1, T_2, \ldots) = (1, 1, 1, \ldots)$ for the level-I staircase; see Fig.3. By applying the above construction to different values of amplitude we obtain an "unfolded" staircase structure for the $A - w$ parameter space. Figs.4,5 show the basic, macroscopic structure of Arnol'd tongues for the steps of levels I and II of the staircase tree. In contrast to the phenomena observed in Chua *et al.* [1986], we have not observed chaotic behavior. Note that the separations of basic steps of level I are approximately integer multiples of the basic angular frequency [3] $w_0 \approx 0.37$ which is the frequency of the response obtained by driving the circuit with a constant signal when the parameter $A \approx -1$.

4. The Period-adding Law

Staircase trees similar to that described in the preceding section have been observed in many physical systems. The order of steps and their size is usually subject to a definite law. Kaneko [1983] formulated a period-adding law in his work on one-dimensional maps. Experimental observations in a second-order circuit [Chua *et al.*,1986] revealed the following period-adding law for winding numbers:

$$q \to q + p \to q + 2p \to \ldots q + np \to \ldots chaos \ldots \to p \tag{4}$$

The interpretation is that by changing the forcing frequency monotonically over a certain range, between any two successive phase-locked states with winding numbers p, q at the same staircase level [4], one can find an infinity of phase-locked states of ascending order, starting from q and leading to a short interval of chaos, before eventually dropping

[3]This general property was observed in many other driven oscillators.

[4]For a more detailed description of levels, refer to the preceding section.

to phase-locked state p. By using numerical simulations on the same circuit, the above law was later confirmed and extended [Luprano & Hasler, 1989] to include also period numbers, and formulated in terms of Farey sums in the following way: Let a subharmonic response be characterized by its winding (w) and period (p) numbers. Suppose $w/p < W/P$ are two successive subharmonics at level k. Then the double staircase of $(k+1)$-st level subharmonics is

$$\frac{w}{p} \rightarrow \frac{w+W}{p+P} \rightarrow \frac{w+2W}{p+2P} \rightarrow \ldots \frac{w+nW}{p+nP} \rightarrow \ldots chaos \rightarrow \frac{W}{P} \tag{5}$$

$$\frac{w}{p} \leftarrow chaos \leftarrow \ldots \frac{nw+W}{np+P} \leftarrow \ldots \frac{2w+W}{2p+P} \leftarrow \frac{w+W}{p+P} \leftarrow \frac{W}{P} \tag{6}$$

We have numerically confirmed the validity of this law (except for the transition to chaos) also in Chua's circuit and will provide a more detailed description of the corresponding subharmonic sequences, based on two-parameter bifurcation diagrams.

Let $W(S_1,\ldots,S_l)$ denote the winding number of the step which is accessed by successively taking S_i steps at level i of the tree ($i = 1,2,\ldots,l$). Since $(S_1,\ldots,S_l,1)$ corresponds to the same location in the tree as $(S_1,\ldots,S_l)$, each step at level l is associated with a unique sequence $(S_1,\ldots,S_l)$ where $S_i > 1$ ($i = 2,3,\ldots$). For example, the encircled step in Fig.3 corresponds to step sequence $(S_1,S_2,S_3,S_4,S_5,S_6) = (2,2,4,3,4,5)$.

It follows that the global hierarchy of winding numbers can be described by the following recurrent relation:

$$\begin{aligned} W(S_1) &= S_1 \quad \forall S_1 \geq 1 \\ W(S_1,\ldots,S_l) &= W(S_1,\ldots,S_{l-1}) + (S_l - 1)W(S_1,\ldots,S_{l-1}-1) \quad \forall l \geq 2 \end{aligned}$$

For example, the step sequence $(S_1,S_2,S_3,S_4,S_5) = (2,4,3,4,3)$ yields the relation $W(2,4,3,4,3) = W(2,4,3,4) + 2W(2,4,3,3)$ which corresponds to the step $\frac{V}{102/79}$ being generated from $\frac{IV}{40/31}$ and $\frac{IV}{31/24}$, where the winding number $102 = 40 + 2 \times 31$; see Fig.3.

As observed from numerical simulations, to every step associated with the sequence $(S_1,\ldots,S_l)$ in the tree, there corresponds its period number, denoted $P(S_1,\ldots,S_l)$, according to the same recurrent equation (but with different 'initial condition'):

$$P(S_1) = 1 \quad \forall S_1 \geq 1$$

$$P(S_1,\ldots,S_l) = P(S_1,\ldots,S_{l-1}) + (S_l - 1)P(S_1,\ldots,S_{l-1}-1) \quad \forall l \geq 2$$

Similarly as above, the reader can check this formula with Fig.3. The condition $P(S_1) = 1$ means that the structure is the same for period numbers in all branches. Another interpretation is that the staircase structure for period numbers lags behind that for winding numbers by one level.

Some explicit formulas for low-level staircases are (we write W_l for $W(S_1,\ldots,S_l)$, similarly P_l):

$$\begin{aligned} W_2 &= S_1 S_2 - S_2 + 1 \\ P_2 &= S_2 \\ W_3 &= S_1 S_2 S_3 - S_1 S_3 - S_2 S_3 - S_1 + 2S_3 + 1 \\ P_3 &= S_2 S_3 - S_3 + 1, \end{aligned}$$

etc.

Interesting relations between period and *torsion numbers* [Uezu & Aizawa, 1982; Parlitz & Lauterborn, 1985] have been found in period-doubling cascades of some two-dimensional oscillators [Parlitz & Lauterborn, 1987; Kurz & Lauterborn, 1988]. Here we give the relationship between winding and period numbers in the above period-adding scenario.

Recall from Fig.4b that Arnol'd tongues, corresponding to level II, form groups with period and winding numbers being related through the equality $W = GP + 1$ where G is the group (serial) number counted from the left. The group number G can be formally defined through equality $G = W - 1$ where W is the winding number of the first step in the level-II staircase. The period number of this step is always 1.

The general relationship between W_l and P_l, at level l, is given by the equality

$$W_l = (S_1 - 1)P_l + R_l$$

where $R_l = R(S_1,\ldots,S_l)$ $(l = 1,2,\ldots)$ is a sequence defined by

$$\begin{aligned} R_1 &\equiv 1, \quad R_2 \equiv 1, \\ R(S_1,\ldots,S_l) &= R(S_1,\ldots,S_{l-1}) + (S_l - 1)R(S_1,\ldots,S_{l-1}-1) \quad \forall l \geq 3 \end{aligned}$$

This is a direct consequence of the above recurrent relations for W_l and P_l. (In particular,

if $(S_l) = (2,2,2,\ldots)$, we obtain $W_l - P_l = F_l$ where F_l is the lth Fibonacci number —in this case $W_l = F_{l+2}$, $P_l = F_{l+1}$, $\quad l = 1,2,\ldots$).
The first few formulas for the relationships between winding and period numbers are therefore

$$\begin{aligned} W_2 &= (S_1 - 1)P_2 + 1 \\ W_3 &= (S_1 - 1)P_3 + S_3 \\ W_4 &= (S_1 - 1)P_4 + S_3 S_4 - S_4 + 1 \end{aligned}$$

...etc.[5] We have observed and verified the validity of the above relations in the staircases up to level VII (Figs.6,7,8).

One can see from the definitions of W_l, P_l, and R_l that the three structures are all based on the same recurrent formula and the only difference is in the initial conditions. Each of the structures is self-similar in that after deleting a finite number of levels we are still left with an infinite structure governed by the same recurrent relations with different initial conditions. The self-similarity translates into the familiar devil's staircase by plotting the ratio W/P versus w/w_0 where w_0 is the natural angular frequency of the circuit at negative constant forcing. By looking at smaller steps in Figs.9,10 we are actually looking at higher-level staicases of the staircase tree.

5. Coexistence of Attractors, Hysteresis, and Period-doubling Phenomenon

It is a well-known fact that Arnol'd tongues in driven oscillators can overlap for certain ranges of parameters, thus indicating the coexistence of attractors. The situation is no different in our particular case, when hysteresis (jumps between coexisting attractors) can sometimes be observed. We have seen in Section 3 (Fig.4) that Arnol'd tongues form groups, each representing a branch in the staircase tree for period numbers. The levels we could observe numerically in different groups can be summarized as follows:

In group 0 : levels I and II
In groups 1,2,3,4 : levels I,II, and IV
In groups 5 and 6 : levels I through VII

One can see in Fig.11 that with increasing frequency high-period solutions become

[5] Note that the relations do not depend on how far we go along level-II staircases.

predominant, which is why higher-level staircases are more readily observable in higher-numbered Arnol'd tongue groups. The coexistence phenomena may be another reason why higher-level staircases are harder to detect in low-numbered groups. Numerous co-existences have been observed, for example, in group 1 where pairs of attractors, e.g., period-1 and period-2, or period-2 and period-3, coexist. Similarly, in group 4, pairs like period-2 and period-5, period-3 and period-7, etc., could be detected. Using the notation of Fig.5, one can conjecture on the coexistences $[\mathrm{II}/(n+1)/n] + [\mathrm{II}/(n+2)/(n+1)]$ in group 1, and $[\mathrm{IV}/(4n+1)/n] + [\mathrm{IV}/(4(2n+1))/(2n+1)]$ in group 4, for all n. This conjecture was verified for all $n \leq 5$. The corresponding initial conditions are listed in Table 1; see also Fig.12.

While the staircases in groups 5 and 6 seem to obey the recurrent formulas of Section 4, a different scenario occurs in groups 2 and 3 in addition to the staircase levels listed above. For instance, the following sequences were observed in group 2:

$$3/1 \rightarrow 6/2 \rightarrow 14/5 \rightarrow 22/8 \rightarrow 30/11 \rightarrow \ldots\infty \rightarrow 8/3$$

between steps 3/1 and 8/3 of level-II staircase, and two stairs

$$6/2 \quad\rightarrow\quad 20/7 \rightarrow 34/12 \rightarrow 48/17 \rightarrow \ldots\infty \rightarrow 14/5,$$

$$14/5 \quad\rightarrow\quad 20/7 \rightarrow 26/9 \rightarrow 32/11 \rightarrow \ldots\infty \rightarrow 6/2$$

between steps 14/5 and 6/2 of the preceding sequence. A traditional 1-parameter representation is shown in Fig.13. In some cases several members of period-doubling sequences can be observed, for example,

$$4/1 \rightarrow 8/2 \rightarrow 16/4 \rightarrow 32/8$$

in group 3, between steps 4/1 and 7/2. Such sequences are very short [6] and have been observed for several steps in different groups. These results suggest that the microscopic arrangement of Arnol'd tongues can be very complicated.

[6]Small step-sizes, e.g., 10^{-4} or less, and long simulation times (> 2000 time units) were used to locate the periodic orbits via the forward Euler integration routine.

5. Conclusions and Future Problems

The hierarchy of the staircase structure of Arnol'd tongues in sinusoidally driven Chua's circuit has been explored numerically and described in terms of recurrent relations. For both winding and period numbers, the staircase trees were found to grow according to the same period-adding law, by starting from different initial conditions.

In view of the generality of vector fields generated by Chua's system, the period-adding law and the relations found between the winding and period numbers can be expected to be universal. In Jensen *et al.* [1983] and Parlitz & Lauterborn [1987] the authors investigate the completeness and fractal dimension of the devil's staircase in the circle map and van der Pol's oscillator. Similar questions about the fractal dimension of the devil's staircase in Chua's circuit should be pursued. Another direction is the exploration of three- and more-parameter bifurcation structures, analogously to Mettin *et al.* [1993].

Because of the highly relaxational character of the Chua system with the parameter values we used, it is possible to use Chua's circuit as an elementary cell in CNN arrays of coupled cells to generate different wave propagation phenomena. Preliminary experiments suggest that if the coupling is strong enough, the staircase structure carries over to two-dimensional lattices. However, if the diffusion coefficient is small, the phenomena seem to be more complex, especially when the diffusion coefficient approaches the values at which wave propagation failure occurs. This and other questions related to a large number of different types of bifurcation phenomena which have not been discussed here will be the subject of future research.

Acknowledgment

This work was supported in part by the Office of Naval Research under grant N00014-89-J-1402 and by the National Science Foundation under grant MIP 91-14168.

References

Anishchenko, V. C., Vadivasova, T. E., Postnov, D. E., Sosnovtseva, O. V., Wu, C. W. & Chua, L. O. [1995] "Dynamics of the non-autonomous Chua's circuit," to appear in *Int.J.Bifurcation and Chaos* **5**(2).

Chua, L. O., Yao, Y. & Yang, Q. [1986] "Devil's staircase route to chaos in a non-linear circuit," *Int.J.Circuit Theory Appl.* **14**, 315–329.

Chua, L. O., Wu, C. W., Huang, A. & Zhong, G-Q. [1993] "A universal circuit for studying and generating chaos — parts I and II," *IEEE Trans. Circuits Syst.* **CAS-40**(10), 732-761.

Cvitanović, P., Shraiman, B., & Söderberg, B. [1985] "Scaling laws for mode lockings in circle maps," *Physica Scripta* **32**, 263–270.

Ding. E. J. & Hemmer, P. C. [1988] "Winding numbers for the supercritical sine circle map," *Physica* **D32**, 153–160.

English, V. & Lauterborn, W. [1991] "Regular window structure of a double-well Duffing oscillator," *Phys. Rev.* **A44**(2), 916–924.

Harmon, L. D. [1961] "Studies with artificial neurons, I: properties and functions of an artificial neuron," *Kybernetik* **1** (Heft 3), 89–101.

Jensen, M. H, Bak, P. & Bohr, T. [1983] "Complete devil's staircase, fractal dimension, and universality of mode-locking structure in the circle map," *Phys. Rev. Lett.* **50**, 1637–1639.

Jensen, M. H, Bak, P. & Bohr, T. [1984] "Transition to chaos by interaction of resonances in dissipative systems. I.Circle maps," *Phys. Rev.* **A30**, 1960–1969.

Kaiser, F. & Eichwald, C. [1991] "Bifurcation structure of a driven, multi-limit-cycle van der Pol oscillator (I) The superharmonic resonance structure," *Int.J.Bifurcation and Chaos* **1**(2), 485–491.

Kaneko, K. [1983] "Transition from torus to chaos accompanied by frequency lockings with symmetry breaking," *Prog. Theor. Phys.* **69**(5), 1427–1442.

Kennedy, M. P. & Chua, L. O. [1986] "Van der Pol and chaos," *IEEE Trans. Circuits Syst.* **CAS–33**(10), 974–980.

Kennedy, M. P., Krieg, K. R. & Chua, L. O. [1989] "The devil's staircase: the electrical engineer's fractal," *IEEE Trans. Circuits Syst.* **CAS–36**(8), 1133–1139.

Kurz, T. & Lauterborn, W. [1988] "Bifurcation structure of the Toda oscillator," *Phys. Rev.* **A37**(3), 1029–1031.

Luprano, J. & Hasler, M. [1989] "More details on the devil's staircase route to chaos," *IEEE Trans. Circuits Syst.* **CAS–36**(1), 146–148.

Madan, R. N., ed. [1993] *Chua's Circuit: A Paradigm for Chaos* (Singapore: World Scientific).

Mandelbrot, B. B. [1977] *Fractals: Form, Chance, and Dimension* (San Francisco,CA: Freeman).

Mettin, R., Parlitz, U. & Lauterborn, W. [1993] "Bifurcation structure of the driven van der Pol oscillator," *Int.J.Bifurcation and Chaos* **3**(6), 1529–1555.

Murali, K. & Lakshmanan, M. [1991] "Bifurcation and chaos of the sinusoidally driven Chua's circuit," *Int.J.Bifurcation and Chaos* **1**(2),369–384.

Murali, K. & Lakshmanan, M. [1992] "Transition from quasiperiodicity to chaos and devil's staircase structures of the driven Chua's circuit," driven Chua's circuit," *Int.J.Bifurcation and Chaos* **2**(3), 621–632.

Murali, K. & Lakshmanan, M. [1993a] "Chaotic dynamics of the driven Chua's circuit," *IEEE Trans. Circuits Syst.* **CAS-40**(1), 836–839.

Murali, K. & Lakshmanan, M. [1993b] "Controlling of chaos in the driven Chua's circuit," J.Circuits, Systems, and Computers **3**(1), 125–137.

Parlitz, U. & Lauterborn, W. [1985] "Resonances and torsion numbers of driven dissipative nonlinear oscillators," *Z. Naturforsch.* **41a**, 605–614.

Parlitz, U. & Lauterborn, W. [1987] "Period-doubling cascades and devil's staircases of the driven van der Pol oscillator," *Phys. Rev.* **A36**(3), 1428–1434.

Pei, L-Q., Guo, F., Wu, S-X. & Chua, L. O. [1986] "Experimental confirmation of the period-adding route to chaos in a nonlinear circuit," *IEEE Trans. Circuits Syst.* **CAS–33**(4), 438–442.

Pérez-Muñuzuri, A., Pérez-Muñuzuri, V., Pérez-Villar, V. & Chua, L. O. [1993] "Spiral waves on a 2-D array of nonlinear circuits," *IEEE Trans. Circuits Syst.* **CAS–40**(11), 872–877.

Rajasekar, S. & Lakshmanan, M. [1988] "Period-doubling bifurcations, chaos, phase-locking and devil's staircase in a Bonhoeffer–van der Pol oscillator," *Physica* **D32**, 146–

152.

Rajasekar, S. & Lakshmanan, M. [1992] "Controlling of chaos in Bonhoeffer–van der Pol oscillator," *Int.J.Bifurcation and Chaos* **2**(1), 201–204.

Uezu, T. & Aizawa, Y. [1982] "Topological character of a periodic solution in three-dimensional ordinary differential equation system," *Prog. Theor. Phys.* **68**(6), 1907–1916.

van der Pol, B. & van der Mark, J. [1927] "Frequency demultiplication," *Nature* **120**(3019), 363–364.

Figure captions

Fig.1. (a) Chua's circuit driven by a sinusoidal current source $\bar{I}(t) = \bar{A}\ cos(\bar{\omega}t)$. (b) Voltage-vs-current characteristic of the nonlinear resistor.

Fig.2. Typical waveform for variable x, corresponding to a period number-1 and winding number-2 solution (green), along with the excitation signal (cyan).

Fig.3. Schematic representation of part of the staircase tree showing branches of increasing levels denoted by Roman numbers. The two numbers (W/P) indicate the corresponding winding and period numbers. The higher-level staircases are entirely between two successive steps of lower-level staircases; the overlap is only used to avoid clutter.

Fig.4. (a) Arnol'd tongues from staircases of level I and II. The period numbers are color-coded as follows: level I: red (period-1); level II: green (period-2), magenta (period-3), yellow (period-4), blue (period-5), cyan (period-6); higher-period solutions are coded as black. Arnol'd tongues between red (period-1) and green (period-2) correspond to level-III, and higher, staircases. (b) Groups 0 through 5 (red through yellow) of tongues for level-II staircases. In each group, at level II, the winding and period numbers are related through the equality $W = GP + 1$, where G is the (serial) group number counted from the left; for instance $W = 3P + 1$ in magenta group.

Fig.5. Three-dimensional view of level-II staircase in group 1. In this case, $W = P + 1 = 3$ (green step), $W = P + 1 = 4$ (magenta), $W = P + 1 = 6$ (blue), etc.

Fig.6. Arnol'd tongues in groups 4 through 8. The color scheme for period numbers is the same as in Fig.4a.

Fig.7. Magnification of a subregion from Fig.6. Levels I through V are coded as red, green, blue, magenta, and white, respectively. The sequences of winding and period numbers for individual tongues are the following (from left): 7/1 (level I, red); 13/2 (level II, green); 20/3, 27/4, 34/5, ..., 69/10 (level III, blue); 137/21, 124/19, 111/17, ..., 33/5, 47/7, 61/9, 75/11 (level IV, magenta); 131/20, 105/16, 79/12, 53/8, 73/11, 93/14, 74/11 (level V, white).

Fig.8. Cross-section from Fig.7 at amplitude $A = 1.048$, showing parts of staircase levels III through VII. The correspondence of winding/period number sequences for individual levels is as follows (from left): 20/3 (level III, blue); 33/5 (level IV, magenta); 53/8, 73/11,

93/14, 113/17, 193/29 (level V, red); 185/28, 152/23, 119/18, 86/13, 179/27, 126/19, 239/36, 166/25 (level VI, green); 271/41, 291/44, 225/34, 199/30 (level VII, white).

Fig.9. Three-dimensional view of the devil's staircase corresponding to Fig.6. The ratio of winding and period numbers (W/P) is plotted as the third coordinate.

Fig.10. Devil's staircase at amplitude $A = 1$.

Fig.11. Structure of Arnol'd tongues for higher frequencies.

Fig.12. Waveforms illustrating coexistence of attractors. The excitation signal I is drawn in cyan. (a) Period-5 waveform of the x variable (green) for the parameter values from Table 1. (b) Period-6 waveform of the x variable at the same parameter values , started from a different initial condition.

Fig.13. Period-2 step gives rise to staircases between steps 3/1 and 8/3.

Table caption

Table 1. Initial conditions and parameter values for coexistence phenomena. Small step-size (5×10^{-5} or less) and long simulation times (2000 time units) should be used to obtain the periodic solutions via the forward Euler method.

A	w	initial conditions (x, y, z)	W/P
0.2400005	0.45	0.024 0.0 -0.023	2/1
0.2400005	0.45	0.02353 0.02082 -0.02286	3/2
0.80852	0.45	0.024 0.0 -0.023	3/2
0.80852	0.45	-3.28727 -2.12605 1.144012	4/3
1.249398181818	0.45	0.024 0.0 -0.023	4/3
1.249398181818	0.45	-3.28727 -2.12605 1.144012	5/4
1.5222	0.45	0.024 0.0 -0.023	5/4
1.5222	0.45	-3.28727 -2.12605 1.144012	6/5
1.6960961	0.45	0.024 0.0 -0.023	6/5
1.6960961	0.45	-3.28727 -2.12605 1.144012	7/6
1.0	1.69109559020408	0.035208 0.755609 0.415944	5/1
1.0	1.69109559020408	0.024 0.0 -0.023	14/3
1.50290273	1.7	-3.28727 -2.12605 1.144012	9/2
1.50290273	1.7	0.024 0.0 -0.023	22/5
1.71402684563758	1.7	-3.28727 -2.12605 1.144012	13/3
1.71402684563758	1.7	0.024 0.0 -0.023	30/7
1.8302928	1.7	0.048188 1.271739 0.8817774	17/4
1.8302928	1.7	0.024 0.0 -0.023	38/9
1.902296	1.7	0.024 0.0 -0.023	21/5
1.902296	1.7	-3.28727 -2.12605 1.144012	46/11

TABLE 1

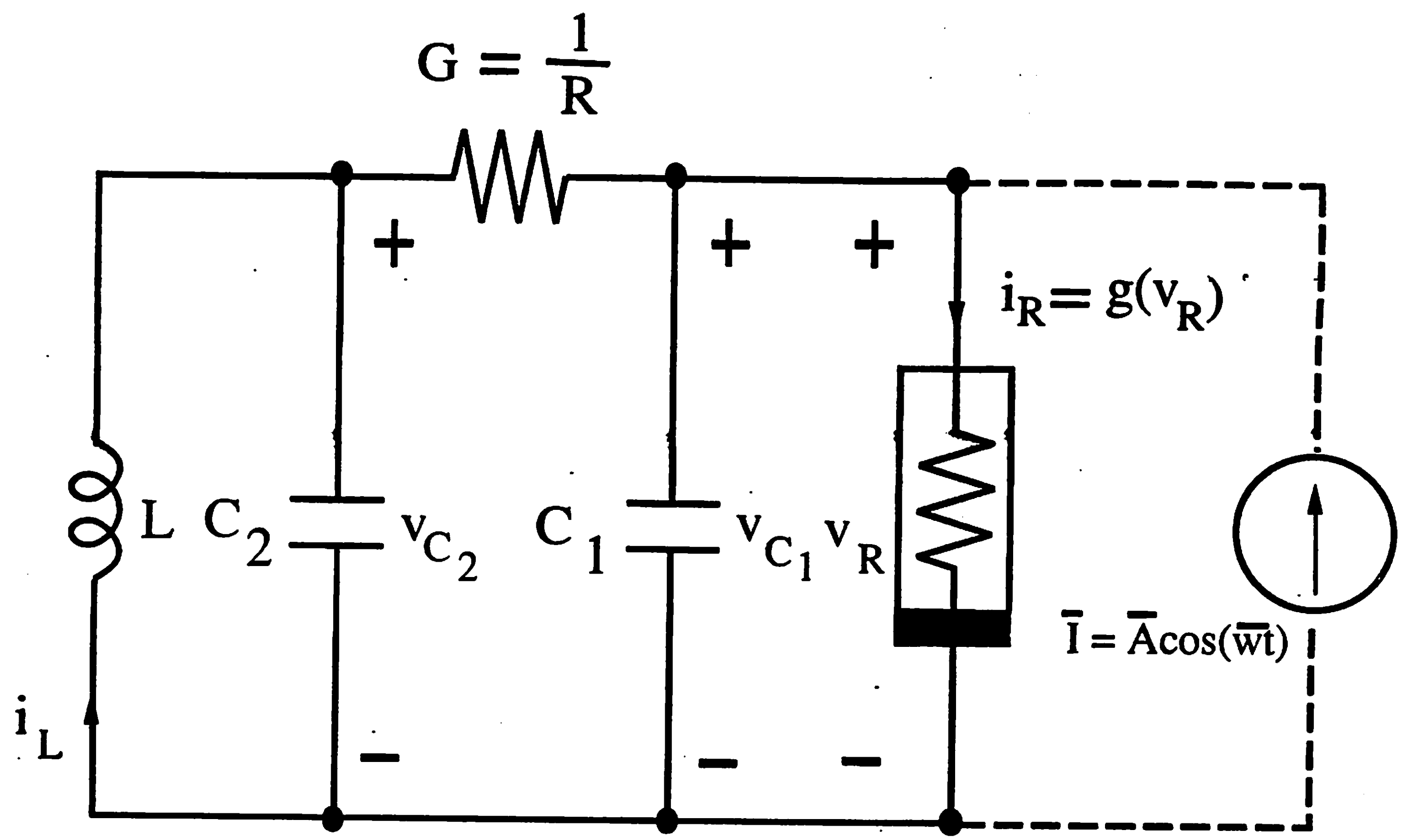

G = 1/R
+
+
+
$i_R = g(v_R)$
L
C_2
v_{C_2}
C_1
v_{C_1}
v_R
$\bar{I} = \bar{A}\cos(\bar{w}t)$
i_L
−
−
−

(a)

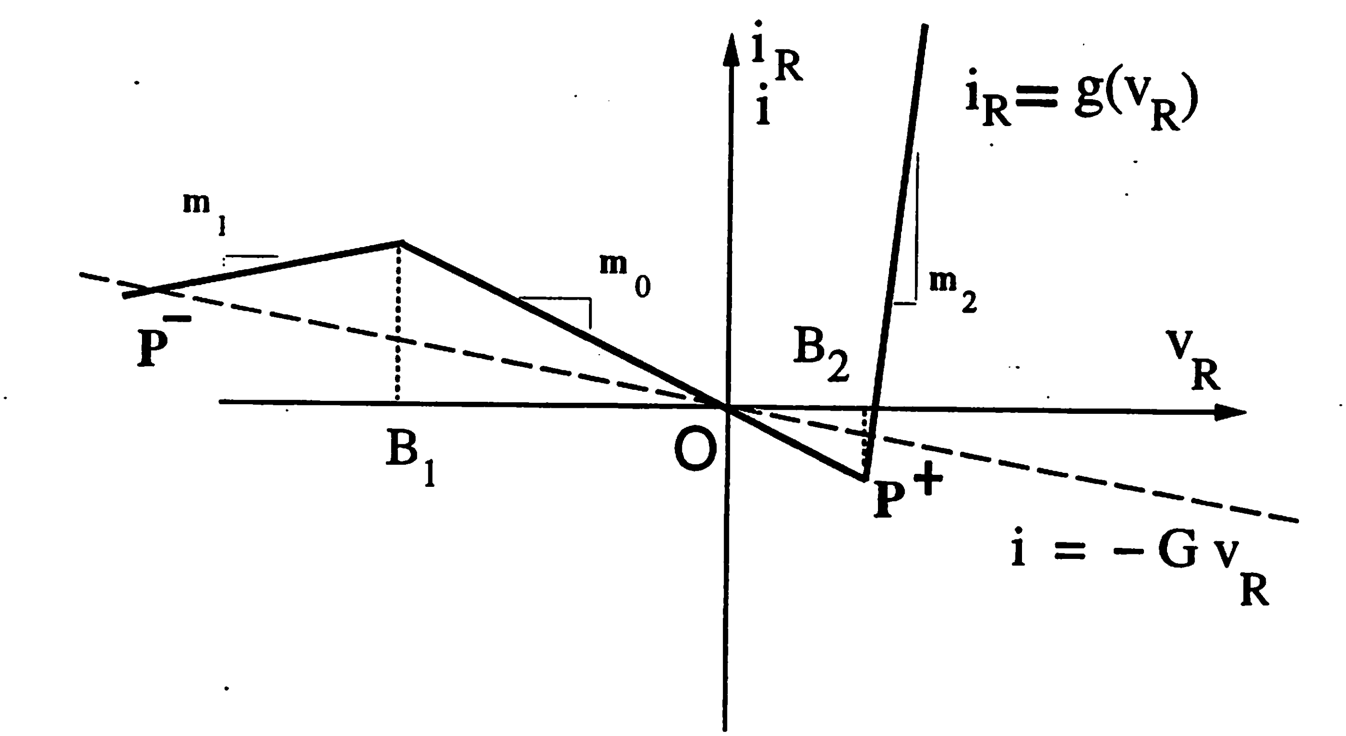

i_R
i
$i_R = g(v_R)$
m_1
m_0
m_2
P^-
B_2
v_R
B_1
O
P^+
$i = -G\,v_R$

(b)

Figure 1

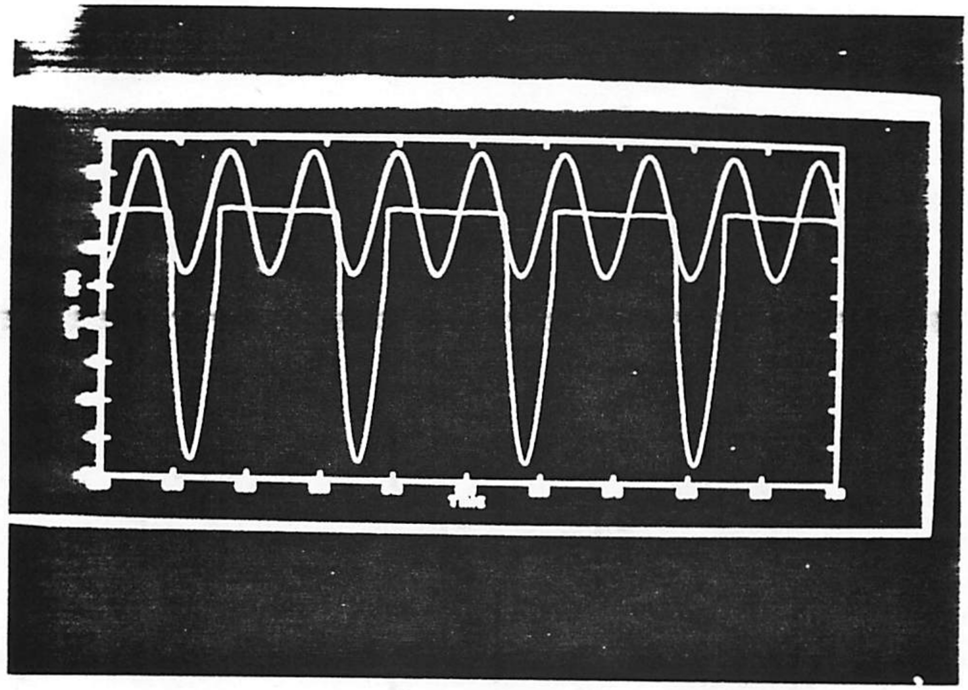

Figure 2

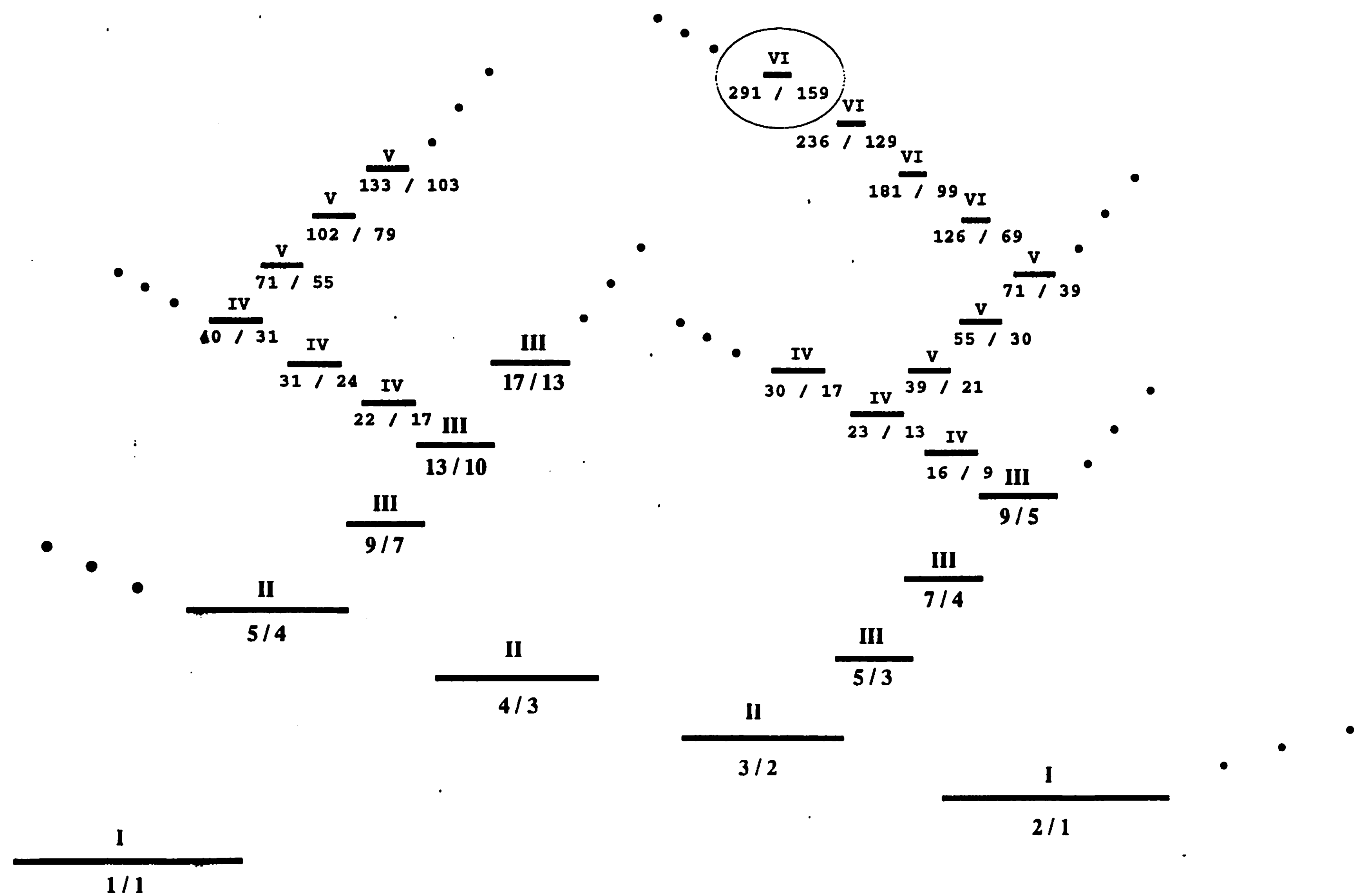

I
1/1
II
5/4
III
9/7
IV
40 / 31
IV
31 / 24
IV
22 / 17
III
13/10
V
71 / 55
V
102 / 79
V
133 / 103
II
4/3
III
17/13
VI
291 / 159
VI
236 / 129
VI
181 / 99
VI
126 / 69
V
71 / 39
V
55 / 30
V
39 / 21
IV
30 / 17
IV
23 / 13
IV
16 / 9
III
9/5
III
7/4
III
5/3
II
3/2
I
2/1

Figure 3

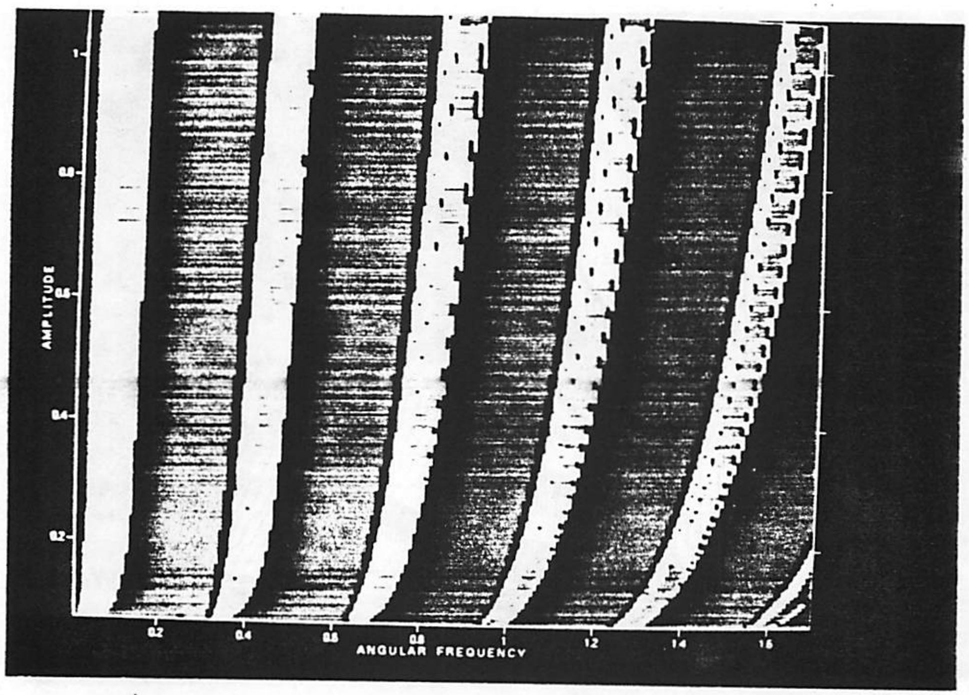

Figure 4a

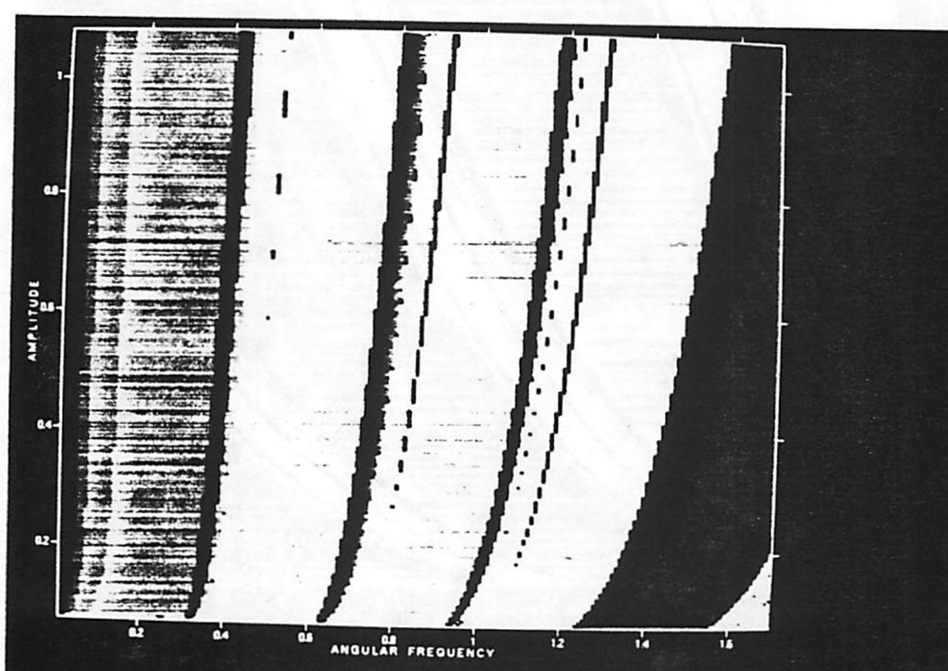

Figure 4b

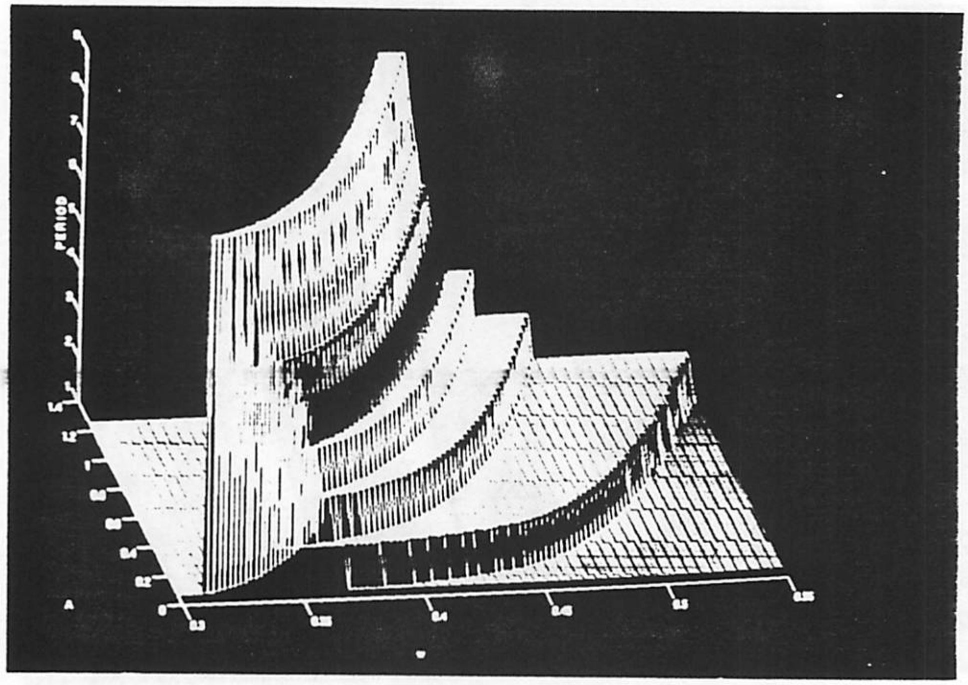

Figure 5

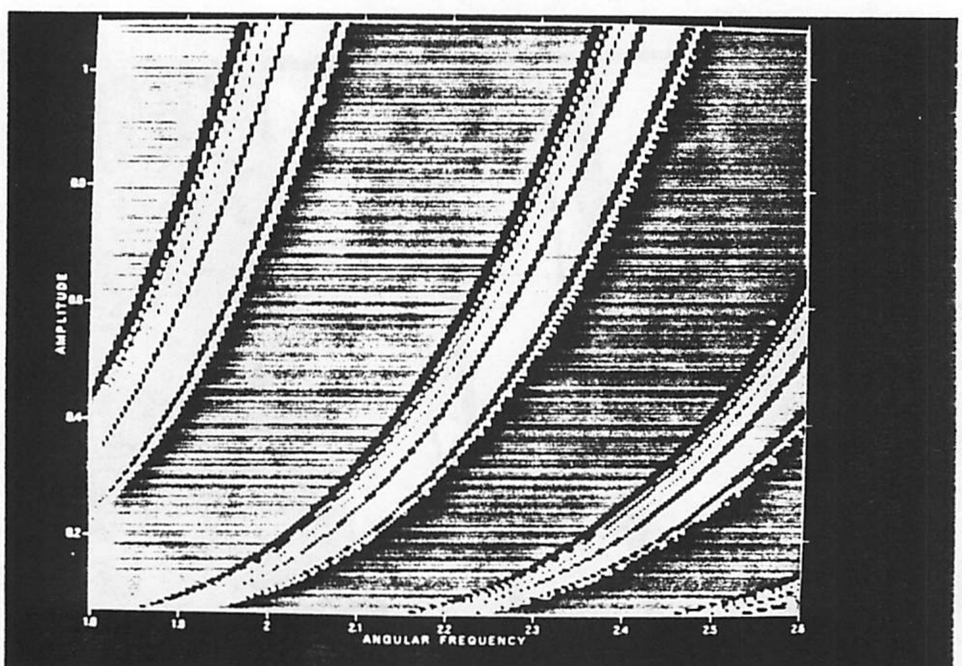

Figure 6

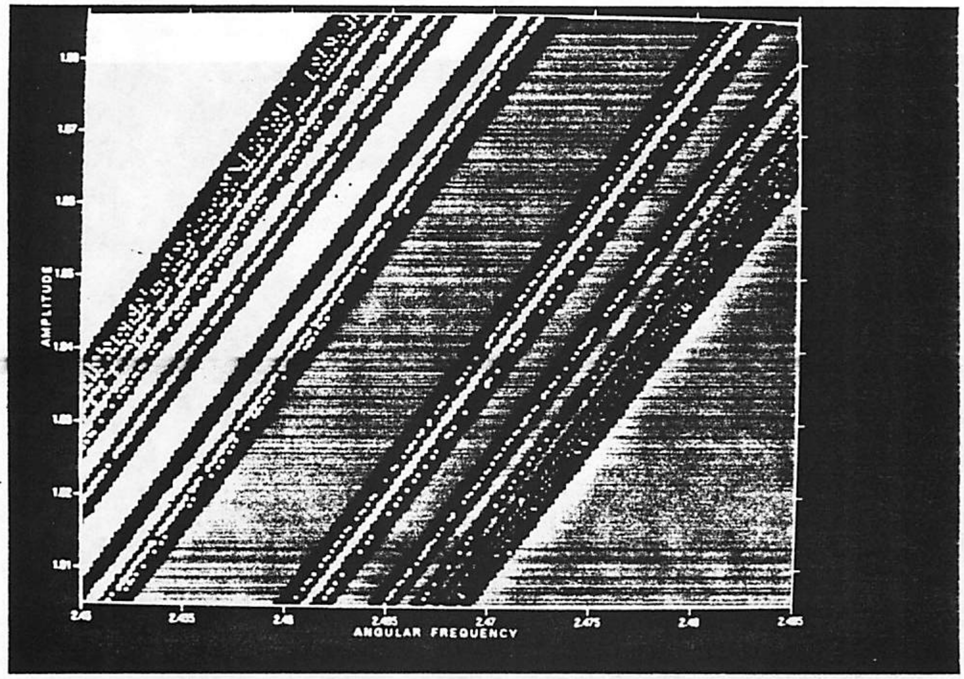

Figure 7

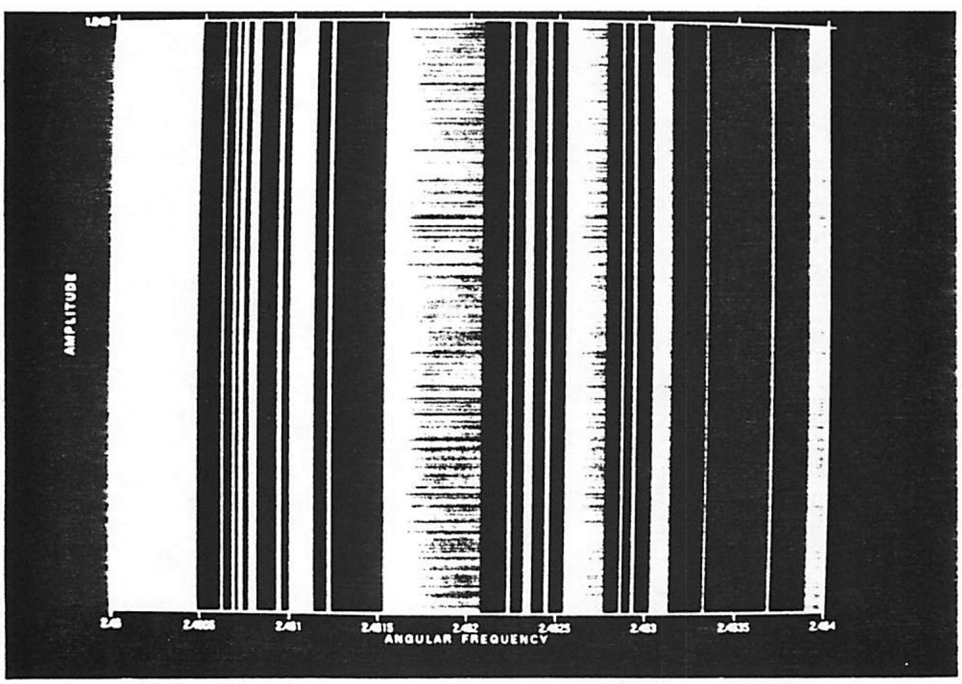

Figure 8

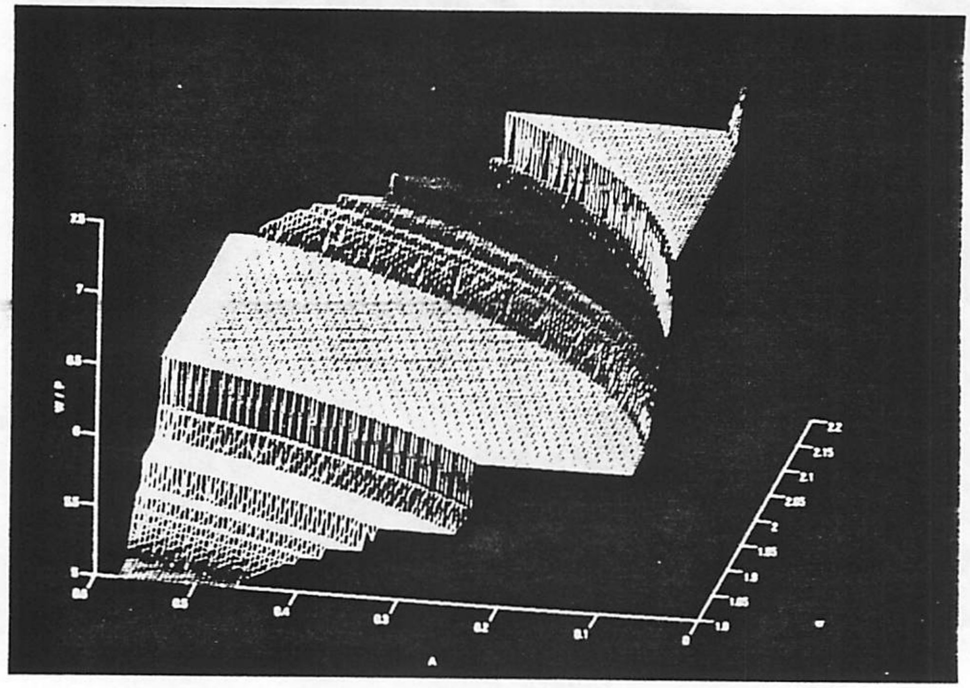

Figure 9

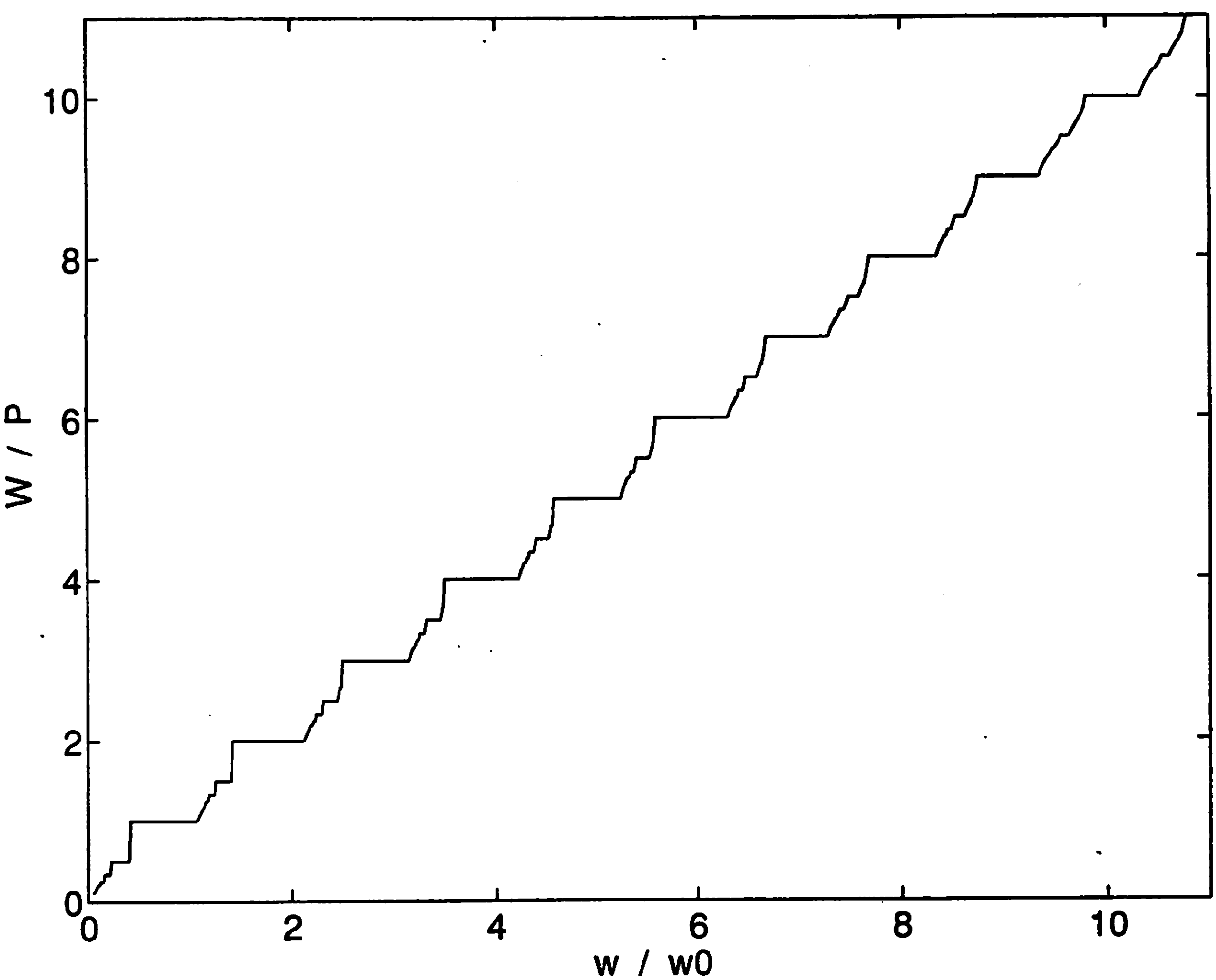

Figure 10

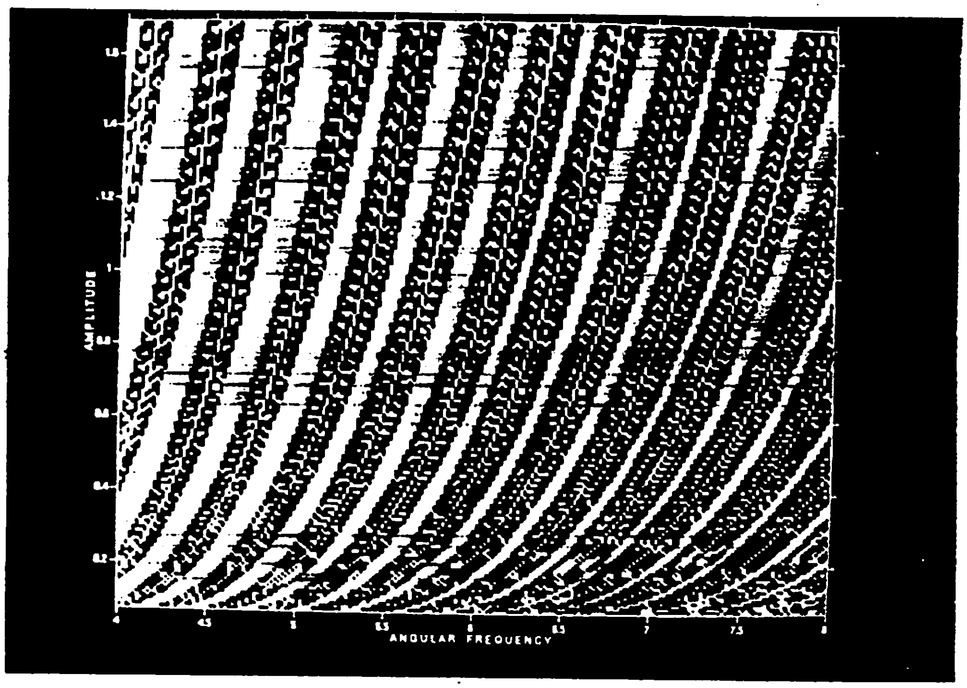

Figure 11

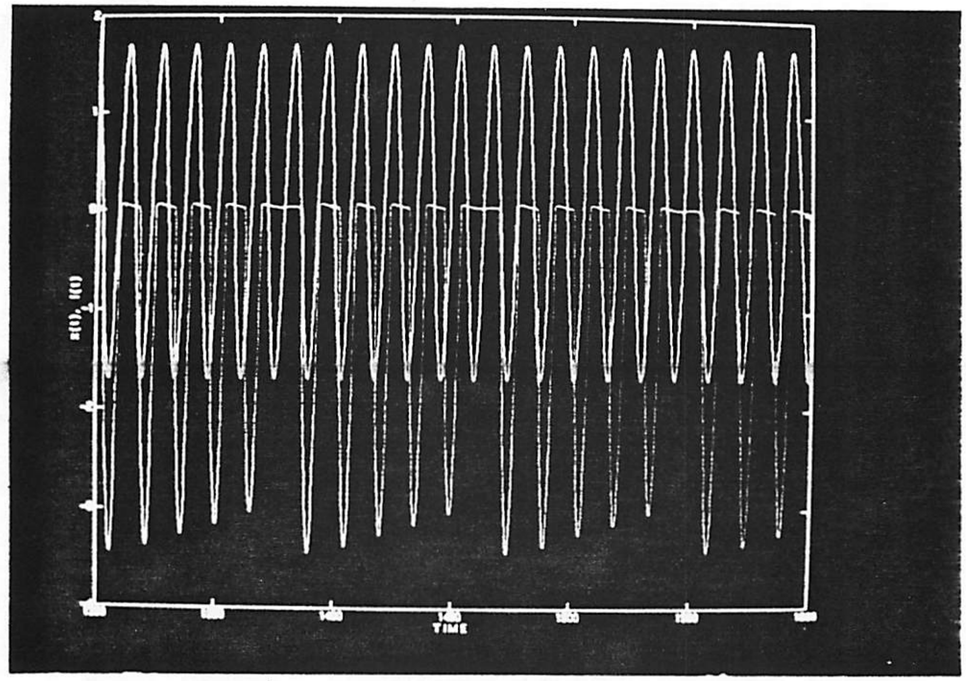

Figure 12a

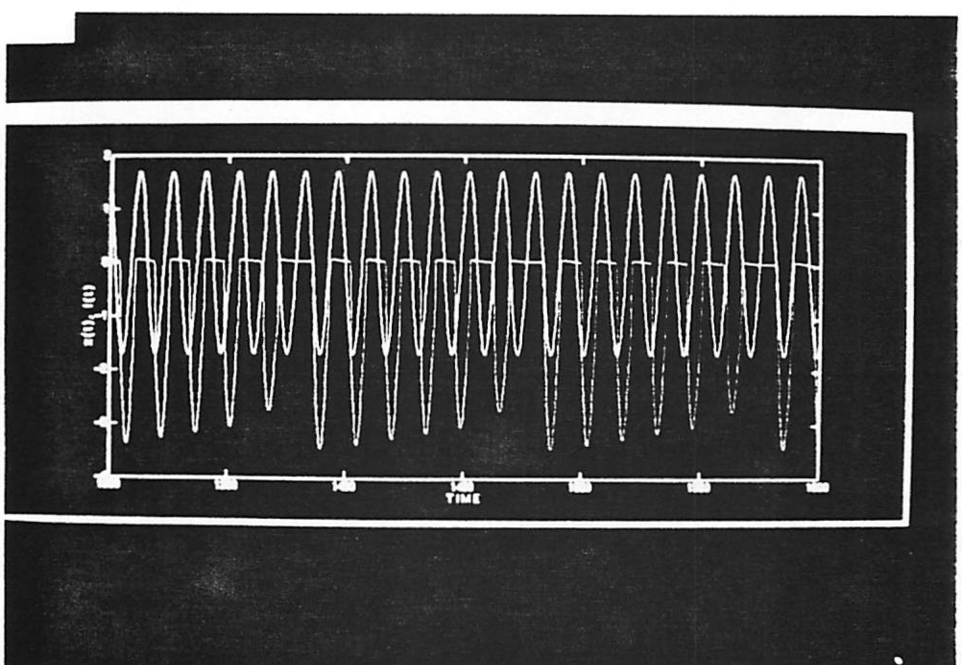

Figure 12b

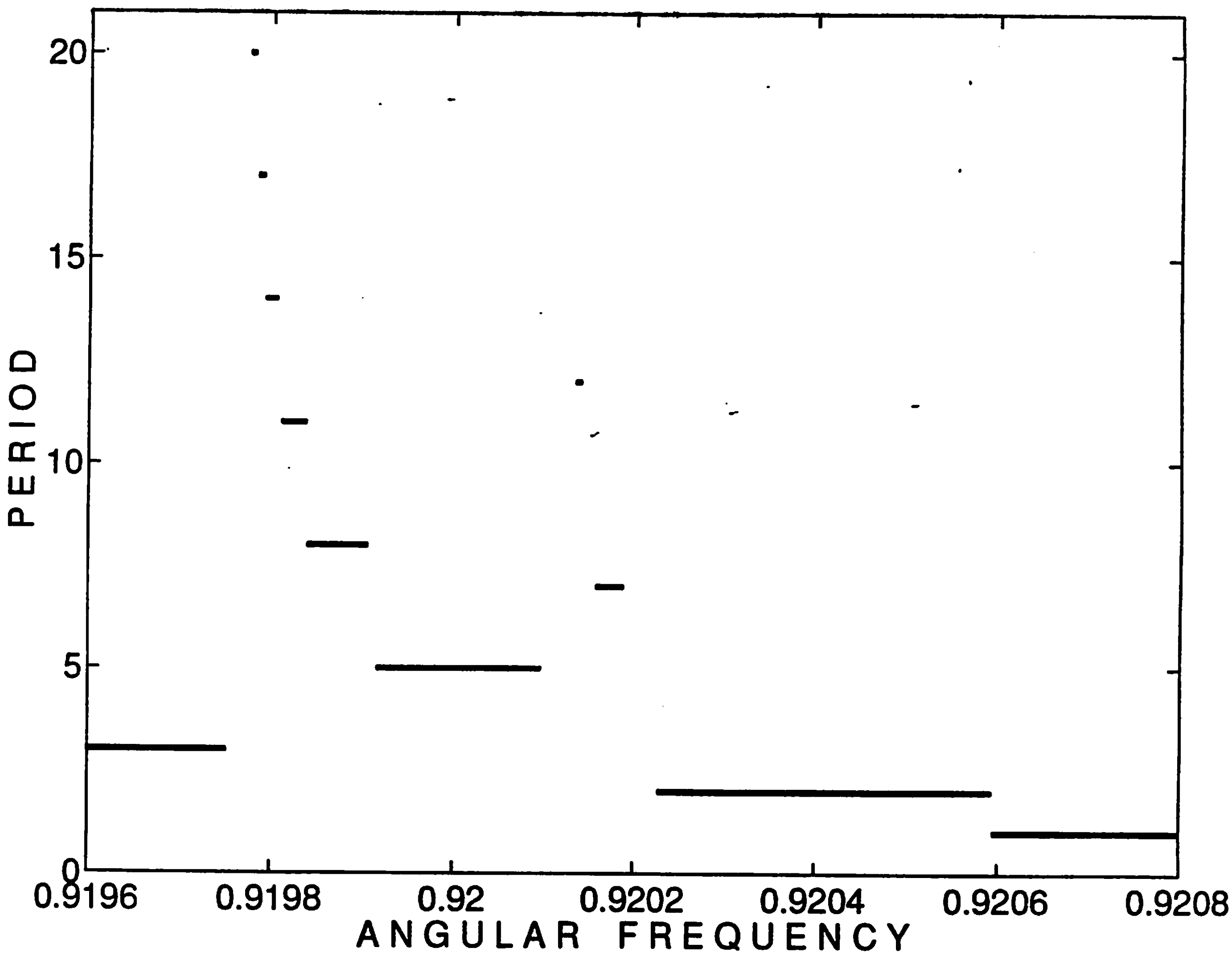
20
15
10
5
0
PERIOD
0.9196
0.9198
0.92
0.9202
0.9204
0.9206
0.9208
ANGULAR FREQUENCY

Figure 13